
Proceedings Paper:
Hotrakool, W. and Abhayaratne, C. orcid.org/0000-0002-2799-7395 (2017) Towards Baseline-Independent Analysis of Compressive Sensed Functional Magnetic Resonance Image Data. In: Digital Signal Processing (DSP), 2017 22nd International Conference on. 2017 22nd International Conference on Digital Signal Processing (DSP), 23-25 Aug 2017, London, United Kingdom. IEEE .

https://doi.org/10.1109/ICDSP.2017.8096065

Towards Baseline-Independent Analysis of Compressive Sensed Functional Magnetic Resonance Image Data

Wattanit Hotrakool and Charith Abhayaratne
Department of Electronic and Electrical Engineering
The University of Sheffield, United Kingdom

***Abstract*—The main task of Functional Magnetic Resonance Imaging (fMRI) is the localisation of brain activities, which depends on the detection of hemodynamic responses in the Blood Oxygenation-Level Dependent (BOLD) signal. While compressive sensing has been widely applied to improve the quality and resolution of MRI in general, its reconstruction noise overwhelms the small magnitude of hemodynamic responses. We propose a new reconstruction algorithm for the compressive sensing fMRI that exploits the temporal redundancy of the data, called Referenced Compressive Sensing, which works well in preserving fMRI analytical features. We also propose the use of the baseline-independent signal for analysis of reconstructed data. It is shown that the baseline-independent reconstructed data from Referenced Compressive Sensing is highly correlated to the lossless data, thus preserving more of the analytical features.**

I. Introduction

One big challenge of Functional Magnetic Resonance Imaging (fMRI) studies is the time required for a subject to remain inside a scanner. Unlike other applications of MRI, fMRI requires a large amount of successive scans per study. The subject is made to remain inside the scanner for a long time, causing anxiety and claustrophobia in the process. To avoid this, fMRI studies usually employ some rapid acquisition techniques such as Echo Planar Imaging (EPI), which dramatically reduces the acquisition time of each scan at the expense of the spatial resolution of the data. One attempt to improve this trade-off between acquisition time and resolution is to incorporate Compressive Sensing (CS) into fMRI acquisition scheme. It is well studied that MRI data is suitable with compressive sensing framework [1], which allows the complete data to be reconstructed from the smaller number compressed measurements. Many works [2], [3], [4], [5] demonstrate the successful application of compressive sensing with clinical MRI and, especially, the dynamic MRI data.

However, even though compressive sensing can greatly improve the trade-off between the acquisition time and resolution of MRI data, the reconstruction is not perfect and the reconstructed data suffers from reconstruction noise. Unlike other MRI techniques, the main analytical feature of fMRI is the variation of the magnitude of voxel's intensity along the temporal axis which signifies the brain activity. This variation, known as a Blood Oxygenation-level Dependent (BOLD) Signal, is due to the correlation between the volume of blood flow and the brain activity. The feature of interest in fMRI is a specific pattern of BOLD signal, called Hemodynamic Response Function (HRF). Because the magnitude of the hemodynamic responses is very small compared to the magnitude of the signal as a whole, the combination of the reconstruction noise and acquisition noise—from environments—presents a tough challenge for the accurate segmentation of the brain active regions.

The most common compressive sensing reconstruction method used to reconstruct the MRI data is the l_1-norm minimisation, which aims to promote the sparsity of the signal. Another reconstruction method for imaging applications is the Total Variation-norm (TV-norm) minimisation. The goal of TV-norm minimisation method is to make the data as smooth as possible rather than as sparse as possible [6], [7]. In practice, however, these methods suffer poor performance when working with MRI data. Instead of doing the reconstruction blindly, many works have shown that by incorporating *a priori* information about the signal into the reconstruction method, the accuracy can be improved greatly [8], [9], [10], [11]. In the spacial case of spatio-temporal signals, such as the case of MRI data, the temporal redundancy can be exploited.

In this work, we propose a novel compressive sensing reconstruction framework for the reconstruction of fMRI data. This reconstruction, referred to as Referenced Compressive Sensing (Referenced CS), exploits the temporal redundancy between each successive scan in order to improve the reconstruction accuracy and to reduce the reconstruction noise. We show that by using the Referenced CS, it is possible to preserve and analyse the analytical features of the reconstructed data. It is also possible to incorporate the Referenced CS with the least squared approximation, giving a dramatic improvement in terms of complexity over the commonly used iterative methods. Moreover, we also show that the reconstruction errors occur in the data reconstructed using Referenced CS is concentrated on the baseline signal, the low frequency variation that does not contain the hemodynamic responses, and these effects can be reduced by using baseline-independent (BI) data for analysis.

II. Proposed method

A. fMRI Data Reconstruction using Referenced Compressive Sensing

In this section we outline a framework to reconstruct the fMRI data from compressive measurements, referred to as the Referenced Compressed Sensing (Referenced CS).

Let the raw data $\mathbf{x} \in \mathbb{R}^n$ denote a frequency domain of a spatial data $\mathbf{u} \in \mathbb{R}^n$, *i.e.*, $\mathbf{x} = \Psi\mathbf{u}$, where Ψ is the Fourier transform basis. Here, to simplify the notations, the spatial data $\mathbf{u}$ is represented as a 1-dimensional vector instead of 3-dimensional matrix which is the actual representation of the data. Given a random encoding operator Φ, the full-length reconstruction $\hat{\mathbf{x}}$ of $\mathbf{x}$ can be obtained from the compressed measurements $\mathbf{y} = \Phi\mathbf{x}$ accurately such that $\|\hat{\mathbf{x}} - \mathbf{x}\|_2 \leq \epsilon$ for a small ϵ.

Here, in *Definition 1*, we define the temporal redundancy between a signal $\mathbf{x}$ and its *correlated reference* signal $\mathbf{r}$.

Definition 1. *A signal* $\mathbf{r}$ *is a correlated reference of* $\mathbf{x}$ *if*

$$\|\mathbf{r} - \mathbf{x}\|_2 \leq \delta, \tag{1}$$

for a sufficiently small δ.

Using the correlated reference $\mathbf{r}$, it is shown in *Proposition 1* that the reconstructed signal $\hat{\mathbf{x}}$ can be obtained accurately.

Proposition 1. *Given a correlated reference* $\mathbf{r} \in \mathbb{R}^n$*, a solution* $\hat{\mathbf{x}}$ *of the problem*

$$\min \|\hat{\mathbf{x}} - \mathbf{r}\|_1 \text{ subject to } \mathbf{\Phi}\hat{\mathbf{x}} = \mathbf{y}, \tag{2}$$

where $\mathbf{y} = \Phi\mathbf{x}$ *is a measurement of* $\mathbf{x} \in \mathbf{X}(R)$*, where*

$$\mathbf{X}(R) = \{\mathbf{x} : \|\mathbf{x} - \mathbf{r}\|_1 \leq R, \mathbf{x} \in \mathbb{R}^n\}, \tag{3}$$

must satisfy

$$\sup \|\mathbf{x} - \hat{\mathbf{x}}\|_2 \leq 2\|\mathbf{x} - \mathbf{r}|_2. \tag{4}$$

Proof. Consider a set of possible solution $\hat{\mathbf{X}}(\mathbf{y}) = \{\mathbf{x} : \mathbf{y} = \Phi\mathbf{x}, \mathbf{x} \in \mathbf{X}(R)\}$. According to the theory of Optimal Recovery, the central algorithm A_c yields the central solution $\hat{\mathbf{x}}^*$ of the solution set. This makes

$$\text{radius}(\hat{\mathbf{X}}(\mathbf{y})) = \sup(\|\mathbf{x} - \hat{\mathbf{x}}^*\|_2 : \mathbf{x} \in \hat{\mathbf{X}}(\mathbf{y})). \tag{5}$$

Because the least-norm solution $\hat{\mathbf{x}} \in \hat{\mathbf{X}}(\mathbf{y})$, therefore

$$\|\hat{\mathbf{x}} - \hat{\mathbf{x}}^*\|_2 \leq \text{radius}(\hat{\mathbf{X}}(\mathbf{y})). \tag{6}$$

From the triangle inequality, $\|\mathbf{x} - \hat{\mathbf{x}}\|_2 \leq \|\mathbf{x} - \hat{\mathbf{x}}^*\|_2 + \|\hat{\mathbf{x}}^* - \hat{\mathbf{x}}\|_2$. This, together with Eq. (5) and Eq. (6), gives

$$\|\mathbf{x} - \hat{\mathbf{x}}\|_2 \leq 2\sup(\|\mathbf{x} - \hat{\mathbf{x}}^*\|_2 : \mathbf{x} \in \hat{\mathbf{X}}(\mathbf{y})). \tag{7}$$

Because $\hat{\mathbf{x}}^*$ is at the centre of $\mathbf{X}(R)$, thus, $\hat{\mathbf{x}}^* = \mathbf{r}$. Therefore, $\|\mathbf{x} - \hat{\mathbf{x}}\|_2 \leq 2\|\mathbf{x} - \mathbf{r}\|_2$. □

It is shown in [12] that the accuracy of the Referenced CS is inversely proportional to δ, with the worst case remains as good as l_1-norm minimisation. In fMRI, the reference $\mathbf{r}$ can be easily obtained from the reconstructed data of its successive volumes.

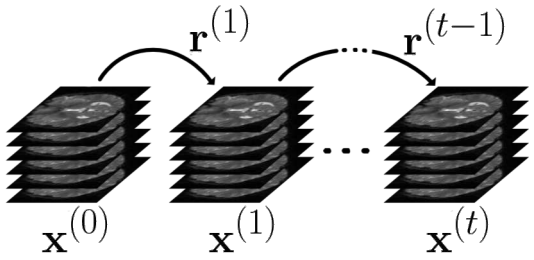

Fig. 1: Referenced CS framework to reconstruct fMRI data

Fig. 1 depicts a configuration that yields the best reconstruction results using the Referenced CS framework. In this configuration, each volume is reconstructed using the previously reconstructed volume as its correlated reference. This ensures that the distance between two signals is kept low and, following the *Proposition 1*, limits the size of the reconstruction error. One drawback of the proposed configuration is that the overall reconstruction quality depends largely on the accuracy of the very first volume. From the practical point-of-view, to maximise the reconstruction quality, the very first volume should be obtained from lossless measurements or using lossless measurements obtained during the scanner calibration as its correlated reference.

It is also possible to incorporate the correlated reference $\mathbf{r}$ into the least square approximation which results in a less complex reconstruction method. In this approach—referred here as Referenced CS with the Least Squares—the reconstructed signal $\hat{\mathbf{x}}$ is obtained from

$$\hat{\mathbf{x}} = \mathbf{r} + \mathbf{\Phi}^{\mathrm{T}}(\mathbf{\Phi}\mathbf{\Phi}^{\mathrm{T}})^{-1}(\mathbf{y} - \mathbf{\Phi}\mathbf{r}). \tag{8}$$

Even though this method yields less accurate reconstructed data, its computation time is only a fraction of other iterative methods, thus making it very suitable for many real-world applications [13].

B. Baseline-independent fMRI data

An observed drawback of the Referenced CS is that the reconstructed data suffers from the loss of dynamic range, due to the use of the temporal information which slows down the variation of the low frequency components of the data, known as the baseline. While the hemodynamic response signal directly corresponds to the stimuli presented to the brain, the baseline is governed by other physical factors unrelated to the stimuli. These hemodynamic responses are relatively small in magnitude, commonly no bigger than 0.5% of the baseline's magnitude. Because the baseline signal does not contain the hemodynamic responses, it is beneficial to separate the baseline signal from the signal containing hemodynamic responses.

In practice, the hemodynamic responses are detected by locating the BOLD signal that shares the same characteristic with the canonical HRF ([14], [15]). Assuming the only two

time-varying functions in the signal are the HRF and the baseline, by removing the baseline function we can obtain the baseline-independent data which contains only the hemodynamic responses.

Let $\mathbf{v}$ denotes a signal of the voxel's intensity on the temporal axis. We can model signal $\mathbf{v}$ as

$$\mathbf{v} = \mathbf{b} + \mathbf{h} + \mathbf{n}, \tag{9}$$

where $\mathbf{b}$ denotes the baseline signal, $\mathbf{h}$ denotes the hemodynamic responses signal, and $\mathbf{n}$ denotes the acquisition noise. Also let $v(t)$, $b(t)$, $h(t)$, and $n(t)$ denote a point each signal $\mathbf{v}$,$\mathbf{b}$,$\mathbf{h}$, and $\mathbf{n}$ at the time instance t, respectively. Because the only signal of interest in fMRI is the responses $\mathbf{h}$, it is desirable to minimise the effects of the baseline $\mathbf{b}$ and the noise $\mathbf{n}$. To remove the effect of the baseline, here we consider strategies for the baseline estimation. Once estimated, the baseline-independent voxel intensity signal $\mathbf{v}'$ can be obtained by

$$\mathbf{v}' = \mathbf{v} - \mathbf{b}. \tag{10}$$

1) Low-pass filtering: A straightforward way to estimate the baseline is to view it as a low-passed signal of $\mathbf{v}$. This approach is especially captivating if we assume that the distribution of $\mathbf{h}$ and $\mathbf{n}$ is identical and independent. Under this assumption, the baseline can be estimated using various low-pass filtering methods. The most direct method is to convolve a low-pass window function, such as Gaussian, Hamming, Blackman, to the signal [16]. Because the window is applied globally, this method of estimation does not perform well with signals containing multi-scale features.

The more localised low-pass filtering can be archived using spatial filtering such as moving average filter [17]. The k-point weighted moving average can compute as

$$b(t) = \sum_i w(i)v(i), \tag{11}$$

where $t - \frac{k-1}{2} \leq i \leq t + \frac{k-1}{2}, i \in \mathbb{I}$, k is an odd integer, and $w(i)$ is the weight function.

2) Curve fitting estimation: A more sophisticated way to estimate the baseline is to fit a baseline function $\mathbf{b}$ to the intensity signal $\mathbf{v}$ such that the error between $\mathbf{b}$ and $\mathbf{v}$ is minimised [18]. Specifically, given that the baseline $\mathbf{b}$ is a degree n polynomial in the form of

$$b(t) = a_n x(t)^n + a_{n-1} + x(t)^{n-1} ... a_1 x(t) + a_0, \tag{12}$$

where $A = \{a_0, ..., a_n\}$ are the coefficients of $\mathbf{b}$,the baseline is obtained from

$$\mathbf{b} = \arg\min_A \|\mathbf{b} - \mathbf{v}\|_2. \tag{13}$$

Eq. (13) can be solved using any optimisation methods. The baseline estimated in this way is a more "whole picture" approach than the filtering method. It works well with the slowly changing nature of the baseline signal, without compromising the high frequency nature of the hemodynamic responses.

III. Experimental results

In this section, we compare the similarity between the BOLD signal from the reconstructed data and the signal from the lossless data. While the common practice to analyse the effects of compressed sensing to the analytical features of fMRI is to compare the final activity maps created from the lossless and reconstructed data, in this work, the analysis of the performance will be done directly on the raw spatio-temporal data. It is with the intention to avoid the effect of the analysis toolboxes, such as Statistical Parametric Mapping (SPM) and FMRIB Software Library (FSL), which normally apply several preprocessing techniques that can dilute the actual effectiveness of the reconstruction methods. The normalised cross-correlation (NCC) is chosen as the similarity metric in this work. NCC provides a relative similarity metric which is consistent with the presence of analytical features. The normalised cross-correlation C between two signal $\mathbf{x}_1$ and $\mathbf{x}_2$ is defined as

$$C(\mathbf{x}_1, \mathbf{x}_2) = \frac{1}{n} \frac{(\mathbf{x}_1 - \mu_1 \mathbf{1})^{\mathrm{T}} (\mathbf{x}_2 - \mu_2 \mathbf{1})}{\sigma_1 \sigma_2}, \tag{14}$$

where n is the length of the signal $\mathbf{x}_1$ and $\mathbf{x}_2$, μ_1,μ_2 and σ_1,σ_2 are the mean and the standard deviation of $\mathbf{x}_1$ and $\mathbf{x}_2$ respectively. The vector $\mathbf{1}$ is the length n vector of all 1s.

The experiment data is reconstructed from the real fMRI data from OpenfMRI project [19] using several reconstruction methods; namely, the naive pseudo-inverse (inverse), the l_1-minimisation (l_1-min), the Total Variation-minimisaiton (TV-min), the proposed Referenced CS (Ref. CS), and the proposed Referenced CS with the Least Squares (Ref. CS/LS). The compressed measurements for these reconstructions are obtained at the under-sampling rate of 0.1, 0.3, and 0.5.

Fig. 2 shows the examples of the reconstructed data using both the Referenced CS and the Referenced CS with the Least Squares, compared to the conventional l_1-minimisation. It can be seen clearly that both the proposed methods preserve far greater details in the reconstructed data than the l_1-minimisation. Objectively, Table I shows the NCC coefficients of each reconstructed data. The reconstruction accuracy of both methods outperforms the l_1-minimisation by a large margin. Considering the sampling rate of 50% for example, the average NCC coefficient of the Referenced CS is 61.89 against 37.97 of the l_1-minimisation, an improvement of 63%. On the other hand, the Referenced CS with the Least Squares has the average NCC coefficient of 59.16, an improvement of 55.8%. While the Referenced CS with the Least Squares cannot outperform the Referenced CS (using l_1-norm objective function), Table II shows that the Referenced CS with the Least Squares can reconstruct the data in just a fraction of the other iterative method.

The results shown so far still contain the baseline signal. We proceed with the comparison between the baseline-dependent (as shown previously) with the baseline-independent data. The estimations of the baseline are done using Blackman window (low-pass filter method), 5-point moving-average (moving

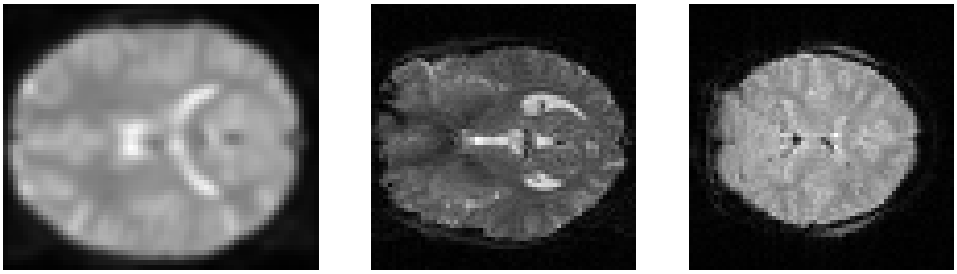

(a) Lossless data

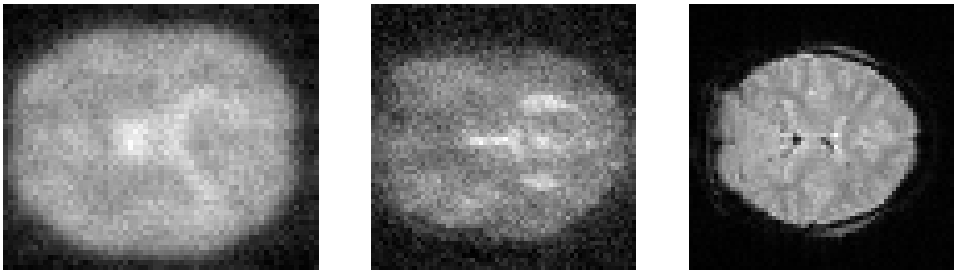

(b) Data reconstructed using l_1-minimisation

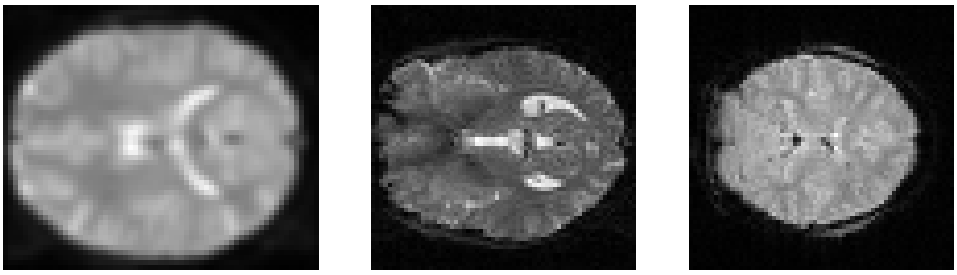

(c) Data reconstructed using Referenced CS

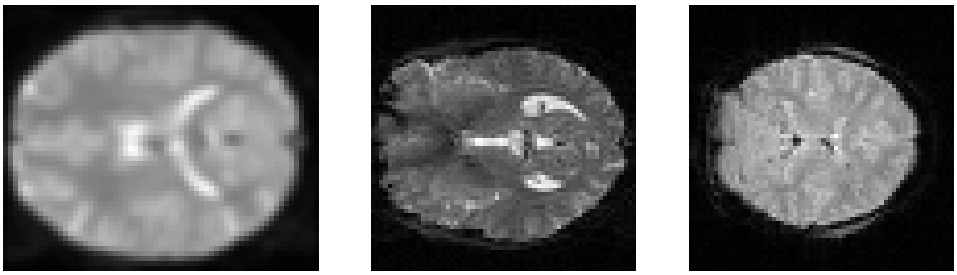

(d) Data reconstructed using Referenced CS with the Least Squares

Fig. 2: Examples of the compressed sensing fMRI data obtained from (a) lossless measurements, (b) reconstructed using the l_1-minimisation, (c) reconstructed using the Referenced CS, and (d) reconstructed suing the Referenced CS with the Least Squares. All examples here are sampled at 50%.

average method), and degree 2 curve fitting (curve fitting method).

Table III compares the NCC coefficients between the baseline-dependent and the baseline-independent data from each reconstruction method. While the data obtained using the conventional l_1-minimisation does not show any benefits from using the baseline-independent analysis, the improvement is noticeable in both the proposed methods. Clearly, the by removing the baseline from the reconstructed data, the correlation between the hemonynamic response signals extracted from the lossless data and the reconstructed data increases in both the Referenced CS and Referenced CS with the Least Squares data. In the case of the Referenced CS, at the sampling rate of 50%, the BI-data has 8.47% higher correlation compared to its baseline-dependent counterpart. The best improvement comes from the use of 5-point moving average. Another interesting observation is that, in baseline-independent analysis, the Referenced CS with the Least Squares performs nearly as good as the iterative Referenced CS.

TABLE I: Normalised Cross-correlation coefficient of fMRI data reconstructed suing different methods

Sampling rate	NCC cooefficient (%)				
	Data 1	Data 2	Data 3	Data 4	Average
l_1-minimisation					
0.1	14.52	11.52	8.57	8.24	10.71
0.3	26.13	24.09	19.36	22.09	22.92
0.5	35.24	36.77	46.10	33.75	37.97
Referenced CS					
0.1	31.10	29.37	32.28	28.35	30.23
0.3	54.19	45.09	45.02	43.47	46.94
0.5	70.48	59.99	58.14	58.96	61.89
Referenced CS with the Least Squares					
0.1	28.68	28.35	32.84	29.90	29.94
0.3	40.51	45.29	47.57	46.15	44.88
0.5	52.14	61.25	61.53	61.72	59.16

TABLE II: Average reconstruction time per volume in seconds

Sampling rate	Time (seconds)			
	Data 1	Data 2	Data 3	Data 4
l_1-minimisation				
0.1	218.91	374.28	206.66	194.34
0.3	391.42	602.31	380.46	310.78
0.5	641.68	874.00	662.47	513.71
Referenced CS				
0.1	214.32	373.63	208.13	194.93
0.3	383.95	579.32	385.86	310.87
0.5	636.43	872.67	660.37	496.87
Referenced CS with the Least Squares				
0.1	0.41	0.53	0.35	0.27
0.3	0.92	1.22	0.77	0.72
0.5	1.21	1.71	1.15	1.08

IV. Conclusions

In this paper, we proposed the Referenced Compressive Sensing reconstruction method, which enables better reconstruction of fMRI data compared to l_1-minimisation. We also propose a solution to the issue of reduced dynamic range of the Referenced CS by removing the baseline from the reconstructed data leading to the baseline-independent analysis of fMRI data. The proposed solution was evaluated against traditional l_1-minimisation method and has shown a great improvement in terms of the higher normalised cross-correlation to the lossless data.

TABLE III: Average Normalised Cross-correlation coefficients (NCC) between the baseline-dependent and baseline-independent data from each reconstruction method. The baseline-independent data are extracted using a) Blackman window, b) 5-pt moving average, and c) curve-fitting.

Sampling rate	Baseline-dependent	Baseline-independent		
		Blackman	5-pt MA	Curve fitting
l_1-minimisation				
0.1	10.71	10.15	10.68	10.44
0.3	22.92	11.50	22.56	22.17
0.5	37.97	36.71	37.23	36.98
Referenced CS				
0.1	30.23	31.03	31.38	30.37
0.3	46.94	52.32	52.41	51.98
0.5	61.89	67.05	67.13	66.02
Referenced CS with the Least Squares				
0.1	29.94	30.82	31.37	30.99
0.3	44.88	48.40	51.85	51.69
0.5	59.16	62.24	66.15	65.30

References

[1] M. Lustig, D.L. Donoho, J.M. Santos, and J.M. Pauly, "Compressed sensing MRI," *IEEE Signal Processing Magazine*, vol. 25, no. 2, pp. 72 –82, March 2008.

[2] M. Lustig, D.L. Donoho, and J.M. Pauly, "Sparse MRI: The application of compressed sensing for rapid MR imaging," *Magnetic Resonance in Medicine*, vol. 58, no. 6, pp. 1182–1195, 2007.

[3] L. Weizman, O. Rahamim, R. Dekel, Y.C. Eldar, and D. Ben-Bashat, "Exploiting similarity in adjacent slices for compressed sensing MRI," in *36th Annual International Conference of the IEEE Engineering in Medicine and Biology Society (EMBC)*, August 2014, pp. 1549–1552.

[4] A. Majumdar, R. Ward, and T. Aboulnasr, "Compressed Sensing Based Real-Time Dynamic MRI Reconstruction," *IEEE Transactions on Medical Imaging*, vol. 31, no. 12, pp. 2253–2266, December 2012.

[5] H. Jung, K. Sung, K.S. Nayak, E.Y. Kim, and J.C. Ye, "k-t FOCUSS: A general compressed sensing framework for high resolution dynamic MRI," *Magnetic Resonance in Medicine*, vol. 61, no. 1, pp. 103–116, 2009.

[6] D. Needell and R. Ward, "Stable Image Reconstruction Using Total Variation Minimization," *SIAM Journal on Imaging Sciences*, vol. 6, no. 2, pp. 1035–1058, 2013.

[7] J. Xu, J. Ma, D. Zhang, Y. Zhang, and S. Lin, "Improved total variation minimization method for compressive sensing by intra-prediction," *Signal Processing*, vol. 92, no. 11, pp. 2614–2623, 2012.

[8] V. Kekatos and G.B. Giannakis, "From sparse signals to sparse residuals for robust sensing," *IEEE Transactions on Signal Processing*, vol. 59, no. 7, pp. 3355–3368, 2011.

[9] J. Scarlett, J. S. Evans, and S. Dey, "Compressed Sensing With Prior Information: Information-Theoretic Limits and Practical Decoders," *IEEE Transactions on Signal Processing*, vol. 61, no. 2, pp. 427–439, January 2013.

[10] C.J. Miosso, R. von Borries, and J.H. Pierluissi, "Compressive Sensing With Prior Information Requirements and Probabilities of Reconstruction in l1-Minimization," *IEEE Transactions on Signal Processing*, vol. 61, no. 9, pp. 2150–2164, 2013.

[11] M.F. Duarte and R.G. Baraniuk, "Kronecker compressive sensing," *IEEE Transactions on Image Processing*, vol. 21, no. 2, pp. 494–504, 2012.

[12] W. Hotrakool and C. Abhayaratne, "Running Gaussian Average-based reconstruction for video compressed sensing," in *2014 IEEE International Conference on Acoustics Speech and Signal Processing (ICASSP)*, 2014.

[13] W. Hotrakool and C. Abhayaratne, "Fast compressed sensing reconstruction using the least squares and signal correlation," in *1st IET Intelligent Signal Processing Conference (ISP)*, December 2013, pp. 1.1–1.1(1).

[14] K.J. Friston, J.T. Ashburner, S.J. Kiebel, T.E. Nichols, and W.D. Penny, *Statistical Parametric Mapping: The Analysis of Functional Brain Images*, Academic Press, 2007.

[15] S. Kim, "Principles of Functional MRI," *University of Pittsburgh Medical School*.

[16] D. A. Barkauskas and D. M. Rocke, "A general-purpose baseline estimation algorithm for spectroscopic data," *Analytica chimica acta*, vol. 657, no. 2, pp. 191–197, January 2010.

[17] Sonali, O. Singh, and R.K. Sunkaria, "ECG signal denoising based on Empirical Mode Decomposition and moving average filter," in *2013 IEEE International Conference on Signal Processing, Computing and Control (ISPCC)*, September 2013, pp. 1–6.

[18] A. F. Ruckstuhl, M. P. Jacobson, R. W. Field, and J. A. Dodd, "Baseline subtraction using robust local regression estimation," *Journal of Quantitative Spectroscopy and Radiative Transfer*, vol. 68, no. 2, pp. 179 – 193, 2001.

[19] "OpenfMRI Project," https://openfmri.org/.